Peer-reviewed version available at *Biomedicines* **2020**, *8*, 213; doi:10.3390/biomedicines8070213

Article

Fluorescent Labeling of Helminth Extracellular Vesicles Using an *In Vivo* Whole Organism Approach

Anders T Boysen [1,a], Bradley Whitehead [1,a], Allan Stensballe[2], Anna Carnerup[3], Tommy Nylander[3], Peter Nejsum [1,4,*]

[1] Department of Clinical Medicine, Aarhus University, Aarhus, Denmark
[2] Department of Health Science and Technology, Aalborg University, Aalborg, Denmark.
[3] Department of Chemistry, Physical Chemistry, Lund University, Lund, Sweden.
[4] Faculty of Veterinary and Agricultural Sciences, The University of Melbourne, Melbourne, Australia
* Correspondence: pn@clin.au.dk; Tel.: +45-50541392
[a] **These authors share co-first authorship**

Abstract: In the last two decades, extracellular vesicles (EVs) from the three domains of life, archae, bacteria and eukaryota, have gained increasing scientific attention. As such, the role of EVs in host-pathogen communication and immune modulation are being intensely investigated. Pivotal to EV research is the determination of how and where EVs are taken up by recipient cells and organs *in vivo*, which requires suitable tracking strategies including labelling. Labelling of EVs is often performed post-isolation which increases risks of non-specific labelling and the introduction of labelling artefacts. Here we exploited the inability of helminths to *de novo* synthesise fatty acids to enable labelling of EVs by whole organism uptake of fluorescent lipid analogues and the subsequent incorporation in EVs. We showed uptake of DOPE-Rhodamine in *Anisakis* spp. and *Trichuris suis* larvae. EVs isolated from supernatant of *Anisakis* spp. labelled with DOPE-Rhodamine were characterised to assess effects of labelling on size, structure and fluorescence of EVs. Fluorescent EVs were successfully taken up by the human macrophage cell line THP-1. This study therefore presents a novel staining method that can be utilized by the EV field in parasitology and potentially across multiple species.

Keywords: Extracellular vesicles, vesicle labelling, vesicle tracking, helminth, proteomics, Cryo – TEM.

1. Introduction

Extracellular vesicles, small membranous vesicles that contain a cargo of bioactive molecules are released from organisms spanning all three domains of life (1,2), including parasitic helminths and their hosts (3,4). The discovery and prediction of miRNAs targeting host genes in EVs released by helminths (5,6) suggests that helminth-derived EVs contribute to host-parasite interactions and may modulate host-immune responses, presenting potential translational applications for helminth EVs (3,4,7–9). Central to the study of the biological function of EVs is accurate determination of cellular uptake or biodistribution. For this, labelling techniques of EVs are required but this is not facile and post-isolation labelling techniques can introduce artefacts, through the co-isolation of micelles (10,11) or modulation of the EV surface (12) thereby obscuring accurate assessment of the mechanisms, rate of EV uptake in host cells and biodistribution *in vivo*.

Expression of known EV proteins tagged with fluorescent proteins, such as green fluorescent protein (GFP), provides a specific method of labelling EVs (13). However, such techniques introduce positive selection of vesicle subtypes, are limited by low fluorescent intensity of EVs, potentially interfere with EV biogenesis via steric hindrance and are unsuitable for labelling of EVs from primary cells or whole organisms (14).

An alternative method for pre-labelling of EVs was demonstrated by the culture of human bladder cancer cell lines in the presence of the fluorescent lipid analogue, 1,2-dioleoyl-sn-glycero-3-phosphoethanolamine-N-lissamine rhodamine B sulfonyl (15). Fluorescent rhodamine B-conjugated lipid incorporation within EV membranes during biogenesis allows for direct isolation of fluorescent EVs, in the absence of dye micelles, for subsequent uptake and biodistribution assays. However, to date, pre-labelling of EVs via fluorescent lipid analogue loading has not been demonstrated for whole organisms.

Parasitic helminths do not synthesise fatty acids and instead acquire lipids and fatty acids from host-tissues, -fluids and/or intestinal content (16). Indeed, many of the proteins within the excretory/secretory products of helminths include lipid-binding proteins for the appropriation of host-derived lipids (17–19). Importantly, helminths do not metabolise fatty acids for energy production, rather, host-derived lipids are used in biosynthesis of cell membranes or egg production (20). Fluorescent lipid analogue uptake has been demonstrated previously for the trematode, *Schistosoma mansoni* (21–23). Therefore, helminths present a highly suitable organism for the assessment of fluorescent lipid analogue labelling strategies of EVs *in vivo*.

This proof-of-concept study aimed to validate the *in vivo* uptake of 1,2-dioleoyl-sn-glycero-3-phosphoethanolamine-N-(lissamine rhodamine B sulfonyl) (DOPE-Rho) in nematodes of two different classes; The larval stage of *Trichuris suis* (L1), a whipworm belonging to Enoplea and *Anisakis* spp. (L3) roundworms belonging to Chromadorea. *T. suis* is a porcine whipworm often employed as a model for *T. trichiura* infection that affects ~ 290 million people globally (24). *Anisakis* spp. are zoonotic parasitic nematodes that include *A. simplex* and *A. pegreffii* (25). *Anisakis* spp. have complex lifecycles including crustaceans and fish as intermediate hosts and marine mammals as the final hosts. They can cause anisakidosis if raw or undercooked fish is consumed, which can cause abdominal pain, nausea, vomiting and potentially anaphylaxis and be fatal in rare cases(26,27). This study assessed the applicability of this technique for labelling of EVs from *Anisakis* spp. through *in vivo* uptake of the fluorescent lipid analogue, DOPE-Rho and the functional application of this method in human THP-1 cell uptake studies.

2. Experimental Section

2.1 T. suis hatching and culture

Embryonated *T. suis* eggs were hatched by incubating in 3.3 v/v % sodium hypochlorite for 2 hour at 37°C with 5% CO_2 and subsequently exchanged to DMEM with penicillin (100U/ml), streptomycin (100µg/ml) and 1 µg/ml ciprofloxacin and incubated for two days at 37°C with 5% CO_2.

2.2 Anisakis spp. harvest and culture

Anisakis spp. were collected from the body cavity of freshly caught herring (*Clupea harengus*) bought from a local vendor. The fish was caught in waters of major fishing areas FAO 27-3b or FAO 27-4b, which meet the criteria for having both intermediate and definite hosts for *Anisakis* spp. Larvae were washed in PBS (37 °C), followed by incubation in PBS with penicillin (100U/ml), streptomycin (100µg/ml) and amphotericin B (250ng/ml,) (Anti/Anti, Thermo Fisher) at 37 °C for 1 hour to prevent microbial contamination.

2.3 Larval uptake of fluorescent lipid analogues in vitro

Hatched *T. suis* (L1) were divided into three groups, first group designated live uptake, second group designated passive uptake and last group a negative control. The group designated passive uptake were placed on dryice for 15 minutes to euthanize the larvae. 4 µM 1,2-dioleoyl-sn-glycero-3-phosphoethanolamine-N-lissamine rhodamine B sulfonyl (DOPE-Rho) (Avanti Polar Lipids) in DMEM were added to the groups except the negative control to which was just added DMEM. They were then incubated for 2 hours. *Anisakis* spp. (L3), were incubated with 0, 1, 4 or 8 µM DOPE-Rho

(Avanti Polar Lipids) for 5 minutes or 16 hours. Larvae were harvested at the indicated time points, washed three times in PBS prior to fixation in 10 % formalin for *T. suis* and 4% paraformaldehyde (PFA) for *Anisakis* spp. T. suis larvae were washed 3 times after fixation and counter-stained with Hoechst-33342 nuclear stain. Larvae were imaged using a Leica DM 2000 LED fluorescent microscope (Leica microsystems, Copenhagen, DK) and images were processed in ImageJ 1.52a (NIH).

2.4 Anisakis spp. in vivo EV labelling

Anisakis spp. L3 larvae were maintained in PBS with Anti/Anti throughout culture at 37 °C and 5% CO_2. Three *Anisakis* spp. larvae per well, were incubated with 0, 1, 4 or 8 µM DOPE-Rho (Avanti Polar Lipids) in PBS with Anti/Anti for 16 hours. The larvae were then washed with PBS to remove excess dye, given new PBS with Anti/Anti and incubated for 48 hours and the supernatant was harvested as conditioned PBS. Dye controls were made in parallel without larvae in the wells and dye solution was directly subjected to EV isolation.

2.5 Anisakis spp. extracellular vesicle isolation

EVs from conditioned PBS were isolated by sequential differential centrifugation: 300x g for 10 minutes, 2000x g for 15 minutes, 10,000x g for 30 minutes followed by 110,000x g (40.800 RPM TI-50 rotor) for 90 minutes to isolate EVs. EVs were washed once by re-suspending the pellet in PBS and centrifuged once more at 110,000x g (40.800 RPM TI-50 rotor) for 90 minutes. Washed EVs were re-suspended in PBS for subsequent characterization and uptake studies. Dye controls were subjugated to the same differential centrifugation. Total protein concentration of intact EVs was assessed using BCA assay as per manufacturer's instructions (Thermo Fisher, Pierce BCA assay). Fluorescence of isolated EVs and dye controls in PBS were assessed using a DS-11 spectrophotometer and fluorometer (DeNovix) with excitation at 525nm and emission 565-615nm.

2.6 Nanoparticle tracking analysis

Extracellular vesicle hydrodynamic radius and concentration was assessed using an NS300 (Malvern Pananalytical). Isolated EVs or dye only controls were diluted in filtered (0.2µm) PBS and analysed immediately hereafter. The following conditions were maintained for all analysis of EVs: particles per frame of 20-100, camera level-15, detection threshold-5 and syringe pump speed of 10µl/s. Three one-minute videos were captured per sample prior to analysis using Nanosight NTA 3.4.003 software. Hydrodynamic size is given as the mode of 3 measurements in nm (±SEM) and concentration as the mean of 3 measurements in particles/ml (±SEM).

2.7 Cryo-transmission electron microscopy

Samples were defrosted and subjugated to a short centrifugation to remove aggregates introduced by freeze thaw cycle with a Qualitron DW-41. Samples were prepared in an automated plunge freezer system (Leica EM GP). A 4 µl drop of sample was dispersed on a glow discharged lacey formvar carbon-coated copper grids (Ted Pella), blotted with a filter paper and then plunged into liquid ethane (approximately −183 °C). The vitrified specimens were thereafter stored in liquid nitrogen (−196 °C) prior to imaging. A Fischione Model 2550 cryo transfer tomography holder was used to transfer the specimen into the electron microscope, JEM 2200FS, equipped with an in-column energy filter (Omega filter), which allows zero-loss imaging. The acceleration voltage was 200kV and energy filtered images were digitally recorded with a TVIPS F416 camera using SerialEM under low dose conditions with a 25 eV slit in place. Images were processed in ImageJ 1.52a (NIH).

2.8 Proteomic analysis of extracellular vesicles

50µl (>10µg total protein) from each sample was lysed in 0.1 % ProteaseMax in 0.1 M TEAB; sonicated for 2 minutes in water sonicator and denaturized for 10 minutes at 60°C and stored at -80°C until

further processed. Protein concentration was estimated by protein absorbance at 280 nm on a Nanodrop 1000 UV-vis spectrophotometer (Thermo Scientific, MA, USA) using the extinction coefficient of bovine serum albumin as a reference (Thermo Scientific Pierce BSA Protein; 2mg/mL). Samples were reduced by incubating with 10 mM tris(2-carboxyethyl)phosphine (Thermo Scientific, MA, USA) and 50 mM chloroacetamide (Sigma-Aldrich, MO, USA) final concentration at 37°C for 30 minutes. The samples were subsequently digested overnight with 1µg of sequencing grade modified trypsin in 0.1 M TEAB (Promega, WI, USA). Samples were acidified with 0.1 % trifluoro acetic acid and reduced by vacuum centrifugation. The reduced samples were dissolved in 30uL 2 % acetonitrile; 0.1 % formic acid; 0.1 % trifluoro acetic acid and sonicated for 5 minutes in water bath. An aliquot corresponding to 200ng of tryptic peptides were used for analysis in triplicate (n=3) for quantitative analysis. The samples were separated on a Dionex RSLC UPLC system (Thermo Scientific, MA, USA) with uPAC 50cm analytical column with precolumn (Pharmafluidics, NL). The samples were loaded at 5 minutes at 10ul per min and the mobile phase was ramped over 30 minutes at a constant flowrate of 700 nL/min from 98 % solvent A (0.1 % formic acid) and 2 % solvent B (0.1 % formic acid in acetonitrile) to 45 % solvent B in 40 minutes. Eluted peptides were directly introduced to the coupled ThermoSci QE HF-X mass spectrometer (ThermoSci; Bremen; DE) by a picotip emitter for electrospray ionization (New objective, MA, USA). The mass spectrometer was operated in positive mode using a data-dependent acquisition method with the following settings: mass range m/z 375-1200; MS1-scan resolution 120,000; MS2-scan resolution 30,000; isolation window m/z 1.6 and NCE 28. Peptide hits were searched against *Anisakis* simplex UniProt protein entries (UP000036680; 20,879 entries; released 05/2019) using standard settings in Maxquant v.1.6.12.0 (28). Proteins of interest were analysed using Blast2Go (29) for BLASTP (NCBI).

2.9 Extracellular vesicle uptake in human macrophage-like THP-1 cells

THP-1 cells (purchased from ATCC) were maintained in RPMI-1640 with 10% FBS and 0.05 mM β-mercaptoethanol at 37 °C and 5% CO_2. Cells were activated with 100ng/ml phorbol 12-myristate-13-acetate (PMA) prior to seeding of 200,000 cells per well in chamber slides for 24 hours. Cells were rested in complete media (without PMA) for a further 24 hours prior to uptake studies. DOPE-Rho labelled EVs were added at low and high dose, 2µg and 8µg total EV protein per well and cells incubated overnight in RPMI with 5% EV-depleted FBS. Unlabeled EVs from *Anisakis* spp. were added at a concentration of 12µg per well as a negative control. Cells were then washed once in PBS, fixed with 10 % formalin prior to washing, counterstaining using Hoechst-33342 nuclear stain and mounting in fluoroshield gold (ThermoFisher). Uptake was assessed using a Leica DM 2000 LED fluorescent microscope (Leica microsystems, Copenhagen, DK). Images were processed in ImageJ 1.52a (NIH).

3. Results

3.1. Fluorescent lipid analogue uptake by T. suis L1 larvae

Hatched *T. suis* L1 larvae were incubated with 4 µM DOPE-Rhod in culture media for 2 hours prior to washing, fixation, nuclear counterstaining and analysis by fluorescent microscopy. Fluorescent lipid was taken up by live larvae although stain intensity varied amongst larvae, all showed strong fluorescence in the mouth region (Fig 1A-B). No unspecific fluorescence was observed in non-labelled control larvae (Fig 1C-D). To determine if uptake was a passive or active process, larvae were killed by freeze thaw and incubated for 2 hours with 4 µM DOPE-Rho and analysed. Fluorescent signal was detected in the mouth region of dead larvae, albeit at a much lower intensity, but in contrast to live larvae fluorescence was not distributed elsewhere (Fig 1E+F).

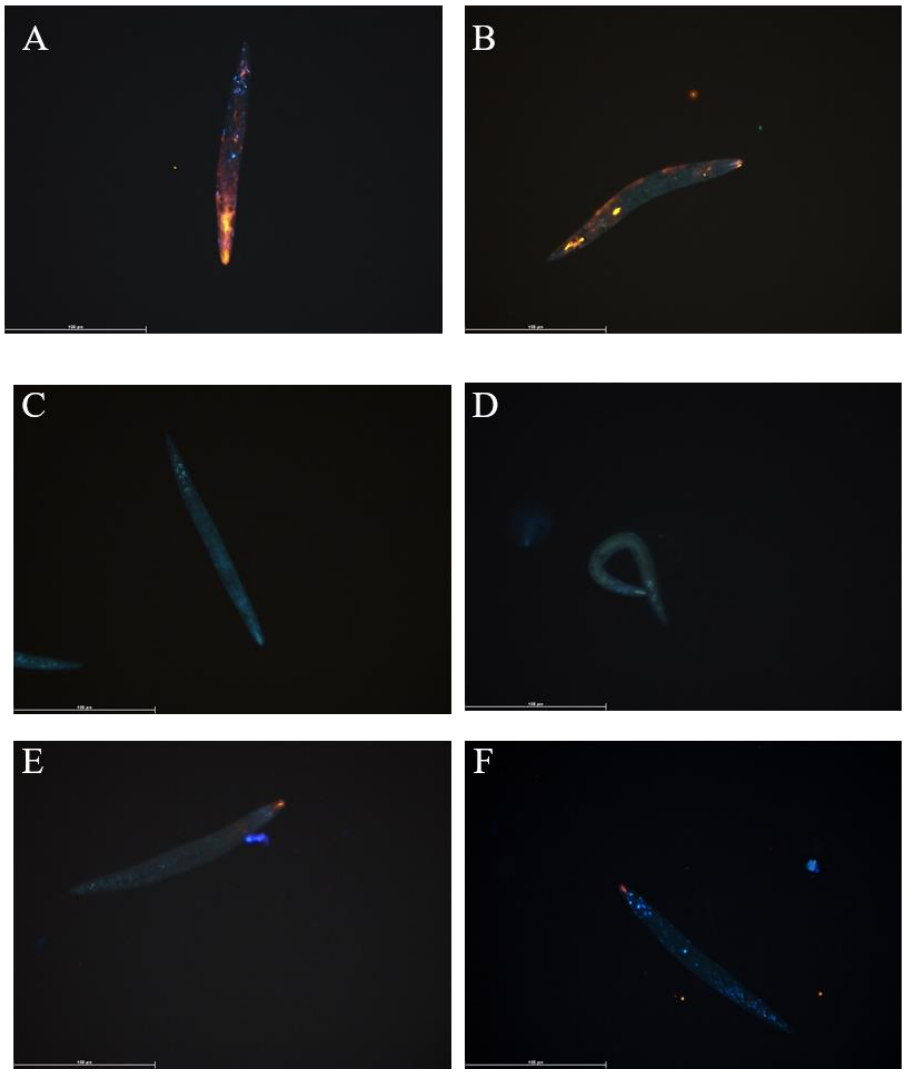

Figure 1. Hatched *T. suis.* (L1) cultured for 4 hours in the presence of 4 μM DOPE-Rho (A+B), control media (C+D) and dead *T.suis* (L1) cultured in 4 μM DOPE-Rho (E+F) prior to washing, fixation with 4% paraformaldehyde and analysis using fluorescence microscopy. Orange=Rhodamine, Blue=Hoechst nuclear stain, Scale bar: 100 μm

3.2. Fluorescent lipid analogue uptake in Anisakis spp.

DOPE-Rho uptake by *Anisakis* spp., assessed by fluorescent microscopy, was time dependent with increasing larvae fluorescence at later time-points (Fig S1+Fig 2). Fluorescence of larvae was dependent upon DOPE-Rho concentration with fluorescent intensity of larvae increasing from 1 to 4 μM DOPE-Rho incubation (Fig 2A-D). However, larvae incubated for 16 hours in 8 μM DOPE-Rho showed a reduced fluorescent intensity (Fig S1E+F).

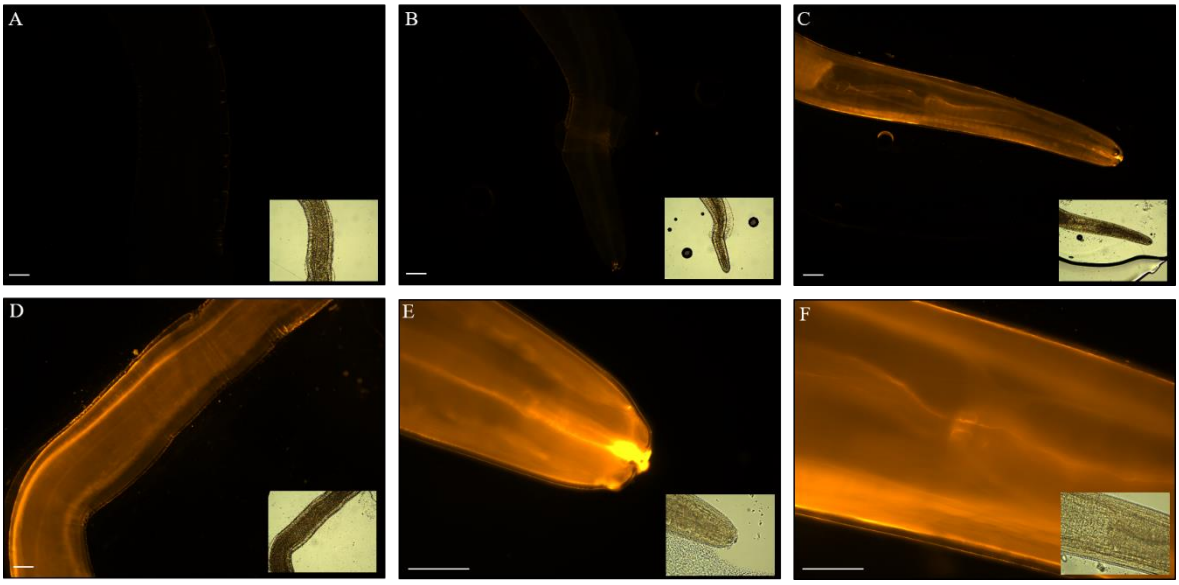

Figure 2. *Anisakis* spp. L3 cultured for 16 hours in the presence of 0 μM (A), 1 μM (B) or 4 μM (C-F) DOPE-Rho prior to washing, fixation with 4% paraformaldehyde and analysis using fluorescence microscopy. Orange=Rhodamine, Scale bar: 100 μm. Corresponding bright field images are inset.

3.3. EVs from *Anisakis spp. characterization and assessment of labelling*

Nanoparticle tracking analysis of non-labelled EVs isolated from *Anisakis* spp. culture media showed EVs released had a modal size of 140.5nm (±7.3nm) with a mean concentration of $2.06x10^{10}$ ($\pm 8.68x10^{8}$) particles/ml (Fig 3A+G). EVs isolated from *Anisakis* spp. incubated with 0, 1, and 4 μM DOPE-Rho had a comparable size distribution, whereas EVs isolated from *Anisakis* spp. Incubated wih 8 μM was shifted towards larger particles (Fig 3A-D).Concentration of particles in the EV sample from 4 μM DOPE-Rho incubated larvae was comparable to that of non-labelled with $1.99x10^{10}$ ($\pm 2.32x10^{8}$) particles/ml. However, a reduction in particle number was observed for 1 μM and a further reduction for 8 μM DOPE-Rho incubated larvae with $1.26x10^{10}$ ($\pm 7.07x10^{8}$) and $4.25x10^{9}$ ($\pm 1.14x10^{8}$), respectively (Fig 3G). The dye controls contained particles comparable to what is present in the diluent PBS and were not fluorescent (Fig 3G+H)

Preprints (www.preprints.org) | NOT PEER-REVIEWED | Posted: 10 July 2020 doi:10.20944/preprints202007.0215.v1

Peer-reviewed version available at Biomedicines 2020, 8, 213; doi:10.3390/biomedicines8070213

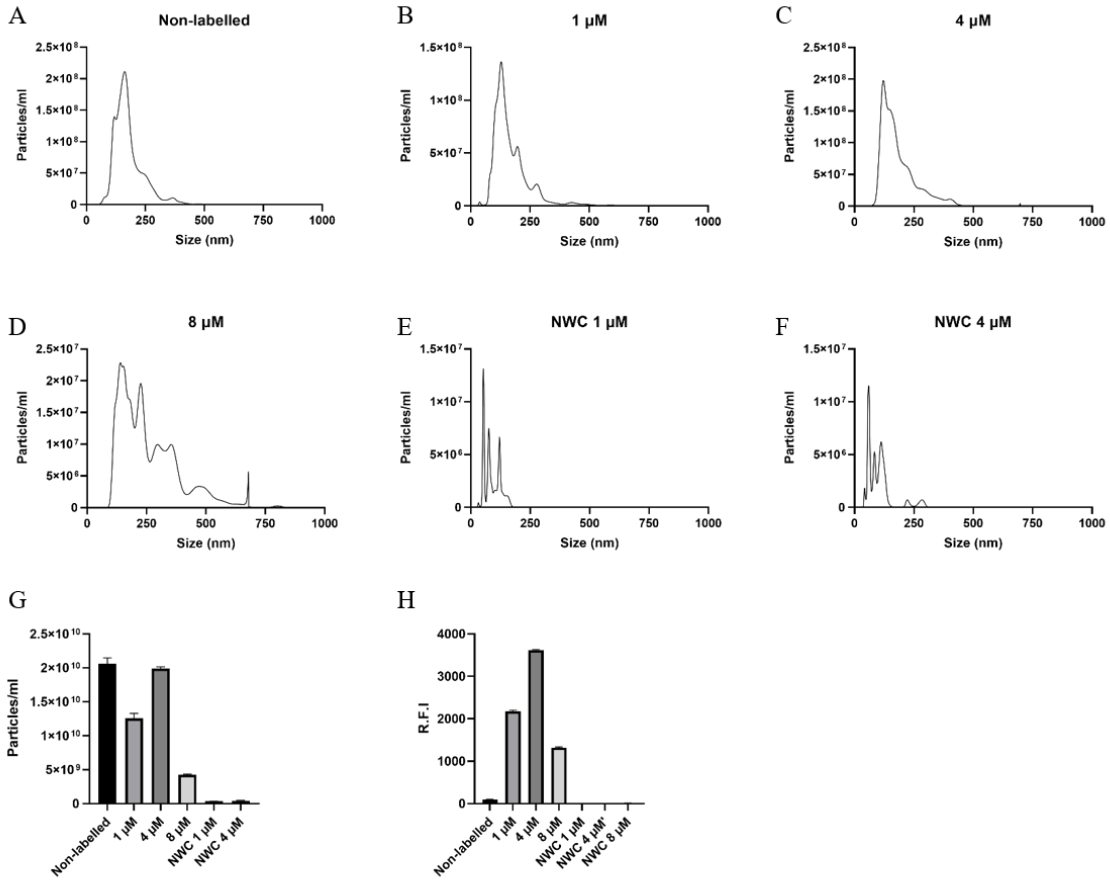

Figure 3. Nanoparticle tracking analysis (NTA) of 100,000x g pellets from untreated *Anisakis* spp. (A), 1 µM (B), 4 µM (C) and 8 µM DOPE-Rho incubated *Anisakis* spp. (D). NTA analysis of no worm dye control (NWC) 1 µM (E) and 4 µM (F) 100,000 x g pellets. Particle number per ml for controls and DOPE-Rho incubated *Anisakis* spp. (G). Relative fluorescent intensity (R:F:I) of 100,000 x g pellets assessed at excitation 525nm and emission 565-615nm (H).

3.4. Cryo-TEM of Anisakis spp.

EVs were heterogeneous in size, and most had a corona of surface molecules (Fig 4). The samples were quite dilute with the highest EV number and absence of aggregates, in the labelled samples derived from larvae incubated with 1 µM DOPE-Rho (Fig 4). The EVs derived from larvae incubated with 4 and 8 µM DOPE-Rho contained a high degree of aggregates and few EVs (Fig S2).

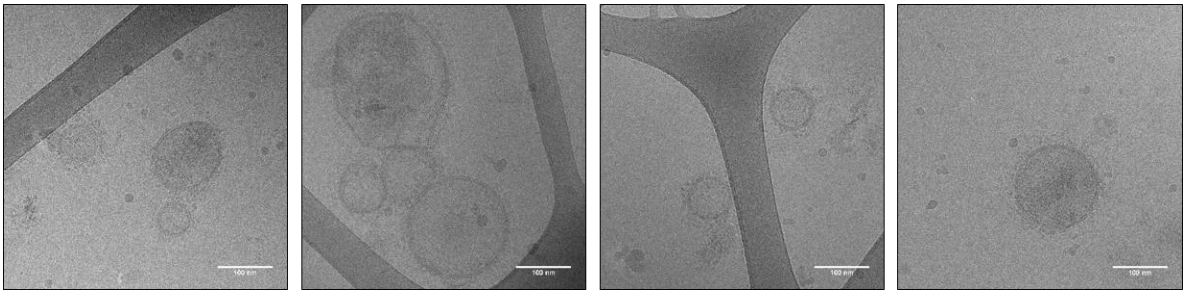

Figure 4. Cryo-TEM images of 1 µM DOPE-Rho labelled *Anisakis* spp. vesicles. Scale bar: 100 nm.

3.5. EVs from Anisakis spp. assessed by quantitative proteomics to identify EV candidate EV markers

Stringent filtering by inclusion criteria requiring at least two unique peptides + razor in triplicates of both day 3 and day 5 harvested EVs. In the absence of prior knowledge of *Anisakis* spp. EV markers, identified proteins, excluding proteases, were compared to selected helminth EV proteomes in the literature (Table 1). Proteins 14-3-3 and HSP70 that are commonly observed in the proteome of mammalian EVs and also the studies referenced in Table 1 were detected in the EV enriched fraction of *Anisakis* spp. GTP binding proteins such as ras-like-protein 3 and ras-like GTP-binding protein RhoA that are implicated in vesicle biogenesis and transport were also detected in *Anisakis* spp. EV enriched samples. Antioxidant protein superoxide dismutase was also detected in EVs from *Anisakis* spp (Table 1).

Table 1. Identified *Anisakis* spp. EV proteins cross-referenced to published helminth EV proteomes.

Accession	Protein	Reference [1]
A0A0M3K8U5	14-3-3	2, 3, 4, 6
A0A0M3K9V2	HSP70	1, 2, 4, 5, 6
A0A0M3IZK3	Tubulin beta	2, 3, 5, 7
A0A0M3K9P2	CBN-exc 4	2, 3, 4, 5 [2]
A0A0M3KB40; A0A0M3J0M4	Actin	1, 5, 6, 7
A0A0M3KFX3	Ras like protein 3	3
A0A0M3J8F3; A0A0M3JD57; A0A0M3K4N2; A0A0M3KAB8; A0A0M3KCN6; A0A158PMY7	Maltase glucoamylase	5
A0A0M3J727; A0A0M3KA60	Histidine acid phosphatase	1, 2, 4, 5 [3]
A0A0M3JAF9	Prostatic acid phosphatase	1, 2, 4 [3]
A0A0M3K4H2	Glutamate dehydrogenase	2, 4, 5
A0A0M3JY91; A0A0M3K219	ATP synthase F1 (alpha+beta subunit)	5
A0A0M3JYW4	RAS-like GTP-binding protein RhoA	2, 5
A0A0M3J718; A0A0M3JZV6	Superoxide dismutase	4
A0A0M3JVA0	ADP ribosylation factor 1	7
A0A0M3JAH0	Pepsin inhibitor	4

[1] *References for homologous proteins identified in EV proteomes of H. polygyrus (1), F. hepatica (2+3), T. muris (4), A. suum (5), S. mansoni (6) and T. circumcincta (7).*

[2] *Chloride channel exc identified in (4), C-exl 1 indentified in (5). Alternative chloride channels identified e.g CLCN7 (2+3).*

[3] *Identified in references as lysosomal acid phosphatase or acid phosphatase.*

3.5. Uptake of DOPE-Rho labelled EVs in THP-1 cells

To further evaluate this EV labelling method, uptake of labelled *Anisakis* spp. EVs was assessed in PMA activated THP-1 cells. As Cryo-EM determined that the EVs from *Anisakis* spp. labelled with 1 µM DOPE-Rho were the purest, this was used for uptake study. Fluorescent EVs were added at 2µg or 8µg (total protein of non-lysed EVs) per well and uptake was assessed using fluorescence microscopy after overnight incubation (Fig 5). Rhodamine fluorescence was detected in a low number of cells incubated with 2µg DOPE-Rho labelled EVs (Fig 5A-C) with the number of rhodamine positive cells increasing at 8µg EV treatment (Fig 5D-F). No rhodamine fluorescent signal was observed in cells treated with 12µg unlabelled EVs (Fig 5G+H) or PBS treated control cells (Fig 5I).

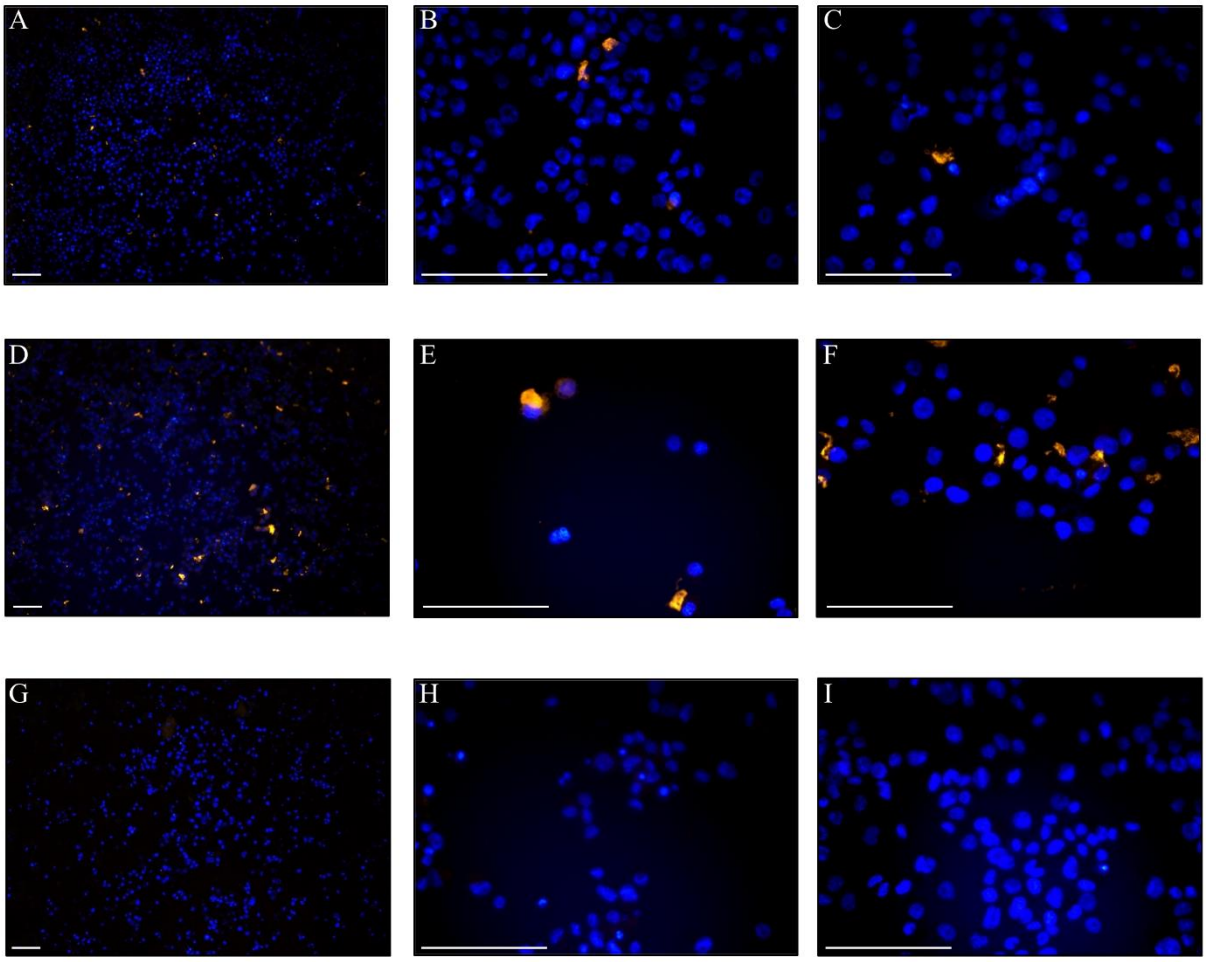

Figure 5. PMA differentiated THP-1 cells incubated overnight with 2µg (A, B and C), or 8µg (D, E and F), 1 µM DOPE-Rho labelled EVs. THP-1 cells incubated with 12µg non-labelled EVs (G and H) or PBS control (I). Orange=Rhodamine labelled EVs, Blue=Hoechst nuclear stain. Scale bar: 100 µm.

4. Discussion

The addition of fluorescent lipid analogue, DOPE-Rho, to culture media was actively taken up *in vivo* and subsequently incorporated by larvae of nematodes from two differing classes of nematodes. Passive uptake was observed in dead *T. suis* larvae albeit reduced when compared to live larvae. Passive uptake is in line with Furlong *et al.* (1992) who saw rapid uptake through the outer membrane of *S. mansoni* and accumulation in the oesophageal gland and gut with headgroup labelled phosphoethanolamine (22). Although the outer surface of nematodes (cuticle) differs from trematodes (tegument) previous studies determined that uptake was mediated via regions of the surface membrane, where lipids can diffuse easily and may explain uptake in dead larvae (35). Helminths produce and secrete several lipid-binding proteins (LBP) (17,19) that are implicated in appropriation of host fatty acids and lipids, which could enable lipid-binding to dead larvae. As per the observations of Furlong *et al.* (1995) in *S. mansoni* cercariae and schistosomula, we also observed accumulation of fluorescent phospholipid at the surface, in the gut (23), and evidence for ingestion of the lipids with staining likely corresponding to the mouth and excretory pore of *Anisakis* spp. While EV subpopulations, such as exosomes and microvesicles, are intensively researched from

mammalian sources (1), little is known about the biogenesis and subpopulations of EV derived from parasites. Nevertheless, a promiscuous labelling as we have performed would be presumed to label every EV subtype secreted from the parasite.

The modal size of vesicles, 140.5nm, harvested from *Anisakis* spp. conditioned media is consistent with the size profile of mammalian small EVs (36) and that previously reported for EVs from *A. suum, T. suis, Fasciola hepatica, Brugia malayi* and *Heligmosomoides polygyrus* (6,37–39). Of note, the incubation of *Anisakis* spp. with the fluorescent lipid analogue, DOPE-Rho, did not alter size distribution of EVs from *Anisakis* spp. at 1-4 μM DOPE-Rho concentration. However, the size distribution of vesicles harvested from 8 μM incubated *Anisakis* spp. indicated that the sample was not as pure and suggested altered release or toxicity at this concentration. The concentration of vesicles isolated from non-labelled and 4 μM DPPE-Rhod labelled were unchanged, however, a small decrease in vesicles was observed in 1 μM DPPE-Rhod EVs. Whilst equal numbers of worms were included per group variations in EV concentration resulting from differences in larvae biomass, and therefore EV production cannot be discounted. However, the greatly reduced number of vesicles in media of 8 μM DOPE-Rho incubated *Anisakis* spp. combined with the reduced lipid uptake in these larvae suggests potential toxicity at this highest concentration. Viability of larvae were only assessed visually, with no reductions in movement observed, but effects on metabolism at this concentration are unknown. Furthermore the larvae were only kept alive until harvest of the EVs was performed, prolonging incubation might have revealed further toxicity of the higher DOPE-Rho concentration eg. 4 and 8 μM.

Using Cryo-TEM we visualized EVs from *Anisakis* spp. with high resolution in their native state with labelling at 1 μM showing the highest purity and EV concentration. Whether the impurities at higher concentrations DOPE-Rho are due to lipid mediating cytotoxicity, and thereby release of dead cells and cuticle, is unknown. The combination of lipid uptake, NTA and cryo-TEM was essential in the determining the optimal concentration of DOPE-Rho used in uptake studies and highlights the risks of relying upon single characterisation techniques in EV biology.

To our knowledge, this study presents the first proteomic study of EVs from *Anisakis* spp. and indeed proteins heavily represented in helminth EV proteomes were identified in *Anisakis* spp. EV enriched samples, including 14-3-3 and HSP70 that are almost ubiquitous in proteomic studies of both mammalian (40,41) and helminth EVs (42,43). Proteases were highly prominent in this analysis, an observation that is consistent with that previously observed for helminth derived EVs (5,6,30,33,34,44). Given the absence of *a priori* knowledge of *Anisakis* spp. EV markers and a lack of commercial antibodies targeting previously proposed EV markers of closely related helminths, we propose that the proteomics approach employed and identification of common helminth EV proteins is sufficient to confirm the presence of intact EVs in isolated fractions, when combined with cryo-electron microscopy.

This proof-of-concept study has shown that labelled fluorescent lipid analogues are internalised by nematodes from two classes. Furthermore, using *Anisakis* spp. as a model system this study has demonstrated that the subsequently released EVs contain fluorescent lipids and their uptake in cells can be assessed by fluorescence microscopy. With the increasing attention on the importance of EVs in host-parasite interaction, this method could not only be used to label all EV subtypes released by nematodes, but may also be applied over a wide range of helminth species. This method could likewise be adapted for the labelling of protozoan EVs, although they both scavenge and synthesize fatty acids *de novo*, fluorescent fatty acids have been shown to be taken up (45–47) and have been employed in the tracking of protozoans intracellularly (47) and trematodes *in vivo* (48). The choice of fluorophore conjugated fatty acid or lipid, uptake duration and concentration should be optimised for each helminth species studied but we propose this may provide a unique method for labelling of EVs *in situ* for subsequent harvest and use in functional assays that is highly suited to helminth biology.

Supplementary Materials: The following are available online at www.mdpi.com/xxx/s1, Figure S1 and S2:

Author Contributions: Conceptualization, ATB, BW and PN.; methodology, ATB, BW and PN.; validation, ATB, BW and AC.; formal analysis, ATB and BW.; investigation, ATB, BW, AS and AC.; resources, AS, TN and PN.; data curation, ATB and BW.; writing—original draft preparation, ATB and BW.; writing—review and editing, ATB, BW, AS, AC, TN and PN.; visualization, BW.; supervision BW and PN.; project administration, PN.; funding acquisition, AS, TN and PN. All authors have read and agreed to the published version of the manuscript.

Funding: This project was supported by the Independent Research Fund Denmark (DFF-6111-00521). The Danish National Mass Spectrometry Platform for Functional Proteomics is acknowledged for MS platform (PRO-MS; grant no. 5072-00007B).

Acknowledgments: The Danish Agency for Science and Higher Education is acknowledged for the funding to Danish National Mass Spectrometry Platform for Functional Proteomics (PRO-MS; grant no. 5072-00007B) enabling parts of this study. We also thank the nCHREM at Lund University where the cryo-TEM experiments were performed. Furthermore we would like to thank professor Holger Jon Møller for technical aid and the Horizon2020 project EVFoundry (H2020-FETOPEN-2016-2017—Project ID: 801367) as a collaboration platform.

Conflicts of Interest: The authors declare no conflict of interest.

References

1. Woith E, Fuhrmann G, Melzig MF. Molecular Sciences Extracellular Vesicles-Connecting Kingdoms. 2019;1–26.

2. Claridge B, Kastaniegaard K, Stensballe A, Greening DW. Post-translational and transcriptional dynamics–regulating extracellular vesicle biology. Expert Rev Proteomics [Internet]. 2019;16(1):17–31. Available from: https://doi.org/10.1080/14789450.2019.1551135

3. Zakeri A, Hansen EP, Andersen SD, Williams AR, Nejsum P. Immunomodulation by helminths: Intracellular pathways and extracellular vesicles. Front Immunol. 2018;9(OCT).

4. Mardahl M, Borup A, Nejsum P. A new level of complexity in parasite-host interaction : The role of extracellular vesicles [Internet]. 1st ed. Vol. 104, Advances in Parasitology. Elsevier Ltd.; 2019. 39–112 p. Available from: http://dx.doi.org/10.1016/bs.apar.2019.02.003

5. Buck AH, Coakley G, Simbari F, McSorley HJ, Quintana JF, Le Bihan T, et al. Exosomes secreted by nematode parasites transfer small RNAs to mammalian cells and modulate innate immunity. Nat Commun [Internet]. 2014;5:1–11. Available from: http://dx.doi.org/10.1038/ncomms6488

6. Hansen EP, Fromm B, Andersen SD, Marcilla A, Andersen KL, Borup A, et al. Exploration of extracellular vesicles from *Ascaris suum* provides evidence of parasite–host cross talk. J Extracell Vesicles [Internet]. 2019;8(1). Available from: https://doi.org/10.1080/20013078.2019.1578116

7. Coakley G, McCaskill JL, Borger JG, Simbari F, Robertson E, Millar M, et al. Extracellular Vesicles from a Helminth Parasite Suppress Macrophage Activation and Constitute an Effective Vaccine for Protective Immunity. Cell Rep [Internet]. 2017 May 23;19(8):1545–57. Available from: https://www.ncbi.nlm.nih.gov/pubmed/28538175

8. Whitehead B, Boysen AT, Mardahl M, Nejsum P. Unique glycan and lipid composition of helminth-derived extracellular vesicles may reveal novel roles in host-parasite interactions. Int J Parasitol [Internet]. 2020; Available from: http://www.sciencedirect.com/science/article/pii/S002075192030120X

9. Eichenberger RM, Sotillo J, Loukas A. Immunobiology of parasitic worm extracellular vesicles. 2018;704–13.

10. Takov K, Yellon DM, Davidson SM. Confounding factors in vesicle uptake studies using fluorescent lipophilic membrane dyes. J Extracell vesicles [Internet]. 2017 Oct 12;6(1):1388731. Available from: https://pubmed.ncbi.nlm.nih.gov/29184625

11. Simonsen JB. Pitfalls associated with lipophilic fluorophore staining of extracellular vesicles for uptake studies. J Extracell Vesicles [Internet]. 2019 Dec 1;8(1):1582237. Available from: https://doi.org/10.1080/20013078.2019.1582237

12. Gangadaran P, Li XJ, Lee HW, Oh JM, Kalimuthu S, Rajendran RL, et al. A new bioluminescent reporter system to study the biodistribution of systematically injected tumor-derived bioluminescent extracellular vesicles in mice. Oncotarget [Internet]. 2017 Nov 18;8(66):109894–914. Available from: https://pubmed.ncbi.nlm.nih.gov/29299117

13. Mittelbrunn M, Gutiérrez-Vázquez C, Villarroya-Beltri C, González S, Sánchez-Cabo F, González MÁ, et al. Unidirectional transfer of microRNA-loaded exosomes from T cells to antigen-presenting cells. Nat Commun [Internet]. 2011;2:282. Available from: https://pubmed.ncbi.nlm.nih.gov/21505438

14. Gangadaran P, Hong CM, Ahn B-C. An Update on *in Vivo* Imaging of Extracellular Vesicles as Drug Delivery Vehicles [Internet]. Vol. 9, Frontiers in Pharmacology . 2018. p. 169. Available from: https://www.frontiersin.org/article/10.3389/fphar.2018.00169

15. Whitehead B, Wu L, Hvam ML, Aslan H, Dong M, Dyrskjøt L, et al. Tumour exosomes display differential mechanical and complement activation properties dependent on malignant state: implications in endothelial leakiness. J Extracell vesicles. 2015;4(1):29685.

16. Brouwers JFHM, Smeenk IMB, van Golde LMG, Tielens AGM. The incorporation, modification and turnover of fatty acids in adult *Schistosoma mansoni*. Mol Biochem Parasitol [Internet]. 1997;88(1):175–85. Available from: http://www.sciencedirect.com/science/article/pii/S0166685197000911

17. McDermott L, Kennedy MW, McManus DP, Bradley JE, Cooper A, Storch J. How Helminth Lipid-Binding Proteins Offload Their Ligands to Membranes: Differential Mechanisms of Fatty Acid Transfer by the ABA-1 Polyprotein Allergen and Ov-FAR-1 Proteins of Nematodes and Sj-FABPc of Schistosomes. Biochemistry [Internet]. 2002 May 1;41(21):6706–13. Available from: https://doi.org/10.1021/bi0159635

18. Alvite G, Esteves A. Lipid binding proteins from parasitic platyhelminthes [Internet]. Vol. 3, Frontiers in Physiology. 2012. p. 363. Available from: https://www.frontiersin.org/article/10.3389/fphys.2012.00363

19. Franchini GR, Pórfido JL, Ibáñez Shimabukuro M, Rey Burusco MF, Bélgamo JA, Smith BO, et al. The unusual lipid binding proteins of parasitic helminths and their potential roles in parasitism and as therapeutic targets. Prostaglandins, Leukot Essent Fat Acids [Internet]. 2015 Feb 1;93:31–6. Available from: https://doi.org/10.1016/j.plefa.2014.08.003

20. Bexkens ML, Mebius MM, Houweling M, Brouwers JF, Tielens AGM, van Hellemond JJ. *Schistosoma mansoni* does not and cannot oxidise fatty acids, but these are used for biosynthetic purposes instead. Int J Parasitol [Internet]. 2019;49(8):647–56. Available from: http://www.sciencedirect.com/science/article/pii/S0020751919301341

21. Keeney DB, Lagrue C, Bryan-Walker K, Khan N, Leung TLF, Poulin R. The use of fluorescent fatty acid analogs as labels in trematode experimental infections. Exp Parasitol [Internet]. 2008;120(1):15–20. Available from: http://www.sciencedirect.com/science/article/pii/S0014489408000921

22. Furlong ST, Thibault KS, Rogers RA. Fluorescent phospholipids preferentially accumulate in sub-tegumental cells of schistosomula of *Schistosoma mansoni*. J Cell Sci. 1992;103(3):823–30.

23. Furlong ST, Thibault KS, Morbelli LM, Quinn JJ, Rogers RA. Uptake and compartmentalization of fluorescent lipid analogs in larval *Schistosoma mansoni*. J Lipid Res [Internet]. 1995 Jan 1;36(1):1–12. Available from: http://www.jlr.org/content/36/1/1.abstract

24. James SL, Abate D, Abate KH, Abay SM, Abbafati C, Abbasi N, et al. Global, regional, and national incidence, prevalence, and years lived with disability for 354 Diseases and Injuries for 195 countries and territories, 1990-2017: A systematic analysis for the Global Burden of Disease Study 2017. Lancet. 2018;392(10159):1789–858.

25. Jeon CH, Kim JH. Pathogenic potential of two sibling species, *Anisakis simplex* (s.s.) and *Anisakis pegreffii* (Nematoda: Anisakidae): in Vitro and in Vivo Studies. Biomed Res Int. 2015;2015.

26. Audicana MT, Kennedy MW. *Anisakis simplex*: From obscure infectious worm to inducer of immune hypersensitivity. Clin Microbiol Rev. 2008;21(2):360–79.

27. Herrador Z, Daschner Á, Perteguer MJ, Benito A. Epidemiological scenario of anisakidosis in Spain based on associated hospitalizations: The tip of the iceberg. Clin Infect Dis. 2019;69(1):69–76.

28. Cox J, Mann M. MaxQuant enables high peptide identification rates, individualized p.p.b.-range mass accuracies and proteome-wide protein quantification. Nat Biotechnol. 2008;26(12):1367–72.

29. Götz S, García-Gómez JM, Terol J, Williams TD, Nagaraj SH, Nueda MJ, et al. High-throughput functional annotation and data mining with the Blast2GO suite. Nucleic Acids Res [Internet]. 2008/04/29. 2008 Jun;36(10):3420–35. Available from: https://pubmed.ncbi.nlm.nih.gov/18445632

30. Cwiklinski K, de la Torre-Escudero E, Trelis M, Bernal D, Dufresne PJ, Brennan GP, et al. The Extracellular Vesicles of the Helminth Pathogen, *Fasciola hepatica*: Biogenesis Pathways and Cargo Molecules Involved in Parasite Pathogenesis. Mol Cell Proteomics [Internet]. 2015/10/20. 2015 Dec;14(12):3258–73. Available from: https://www.ncbi.nlm.nih.gov/pubmed/26486420

31. de la Torre-Escudero E, Gerlach JQ, Bennett APS, Cwiklinski K, Jewhurst HL, Huson KM, et al. Surface molecules of extracellular vesicles secreted by the helminth pathogen *Fasciola hepatica* direct their internalisation by host cells. PLoS Negl Trop Dis [Internet]. 2019 Jan 18;13(1):e0007087–e0007087. Available from: https://www.ncbi.nlm.nih.gov/pubmed/30657764

32. Eichenberger RM, Talukder MH, Field MA, Wangchuk P, Giacomin P, Loukas A, et al. Characterization of *Trichuris muris* secreted proteins and extracellular vesicles provides new insights into host–parasite communication. J Extracell Vesicles [Internet]. 2018;7(1). Available from: https://doi.org/10.1080/20013078.2018.1428004

33. Sotillo J, Pearson M, Potriquet J, Becker L, Pickering D, Mulvenna J, et al. Extracellular vesicles secreted by *Schistosoma mansoni* contain protein vaccine candidates. Int J Parasitol [Internet]. 2016;46(1):1–5. Available from: http://dx.doi.org/10.1016/j.ijpara.2015.09.002

34. Tzelos T, Matthews JB, Buck AH, Simbari F, Frew D, Inglis NF, et al. A preliminary proteomic characterisation of extracellular vesicles released by the ovine parasitic nematode, *Teladorsagia circumcincta*. Vet Parasitol [Internet]. 2016;221:84–92. Available from: http://www.sciencedirect.com/science/article/pii/S0304401716300619

35. Redman CA, Kusel JR. Distribution and biophysical properties of fluorescent lipids on the surface of adult *Schistosoma mansoni*. Parasitology. 1996;113(2):137–43.

36. Jeppesen DK, Hvam ML, Primdahl-Bengtson B, Boysen AT, Whitehead B, Dyrskjøt L, et al. Comparative analysis of discrete exosome fractions obtained by differential centrifugation. J Extracell vesicles. 2014;3(1):25011.

37. Simbari F, McCaskill J, Coakley G, Millar M, Maizels RM, Fabriás G, et al. Plasmalogen enrichment in exosomes secreted by a nematode parasite versus those derived from its mouse host: Implications for exosome stability and biology. J Extracell Vesicles. 2016;5(1).

38. Hansen EP, Kringel H, Williams AR, Nejsum P. Secretion of RNA-Containing Extracellular Vesicles by the Porcine Whipworm, *Trichuris suis*. J Parasitol [Internet]. 2015 Jun 1;101(3):336–40. Available from: https://doi.org/10.1645/14-714.1

39. Zamanian M, Fraser LM, Agbedanu PN, Harischandra H, Moorhead AR, Day TA, et al. Release of Small RNA-containing Exosome-like Vesicles from the Human Filarial Parasite *Brugia malayi*. PLoS Negl Trop Dis [Internet]. 2015 Sep 24;9(9):e0004069–e0004069. Available from: https://pubmed.ncbi.nlm.nih.gov/26401956

40. Niel G Van, Angelo GD, Raposo G. Shedding light on the cell biology of extracellular vesicles. Nat Publ Gr [Internet]. 2018;19(4):213–28. Available from: http://dx.doi.org/10.1038/nrm.2017.125

41. Jeppesen DK, Nawrocki A, Jensen SG, Thorsen K, Whitehead B, Howard KA, et al. Quantitative proteomics of fractionated membrane and lumen exosome proteins from isogenic metastatic and nonmetastatic bladder cancer cells reveal differential expression of EMT factors. Proteomics. 2014;14(6):699–712.

42. Eichenberger RM, Sotillo J, Loukas A. Immunobiology of parasitic worm extracellular vesicles. Immunol Cell Biol [Internet]. 2018 Aug 1;96(7):704–13. Available from: https://doi.org/10.1111/imcb.12171

43. Marcilla A, Trelis M, Cortés A, Sotillo J, Cantalapiedra F, Minguez MT, et al. Extracellular Vesicles from Parasitic Helminths Contain Specific Excretory/Secretory Proteins and Are Internalized in Intestinal Host Cells. PLoS One [Internet]. 2012 Sep 24;7(9):e45974. Available from: https://doi.org/10.1371/journal.pone.0045974

44. Eichenberger RM, Ryan S, Jones L, Buitrago G, Polster R, de Oca MM, et al. Hookworm secreted extracellular vesicles interact with host cells and prevent inducible colitis in mice. Front Immunol. 2018;9(APR):1–14.

45. Stevens TL, Gibson GR, Adam R, Maier J, Allison-Ennis M, Das S. Uptake and cellular localization of exogenous lipids by *Giardia lamblia*, a primitive eukaryote. Exp Parasitol. 1997;86(2):133–43.

46. Gibson GR, Ramirez D, Maier J, Castillo C, Das S. *Giardia lamblia*: Incorporation of free and conjugated fatty acids into glycerol-based phospholipids. Exp Parasitol. 1999;92(1):1–11.

47. Charron AJ, Sibley LD. Host cells: Mobilizable lipid resources for the intracellular parasite *Toxoplasma gondii*. J Cell Sci. 2002;115(15):3049–59.

48. Keeney DB, Lagrue C, Bryan-Walker K, Khan N, Leung TLF, Poulin R. The use of fluorescent fatty acid analogs as labels in trematode experimental infections. Exp Parasitol. 2008;120(1):15–20.

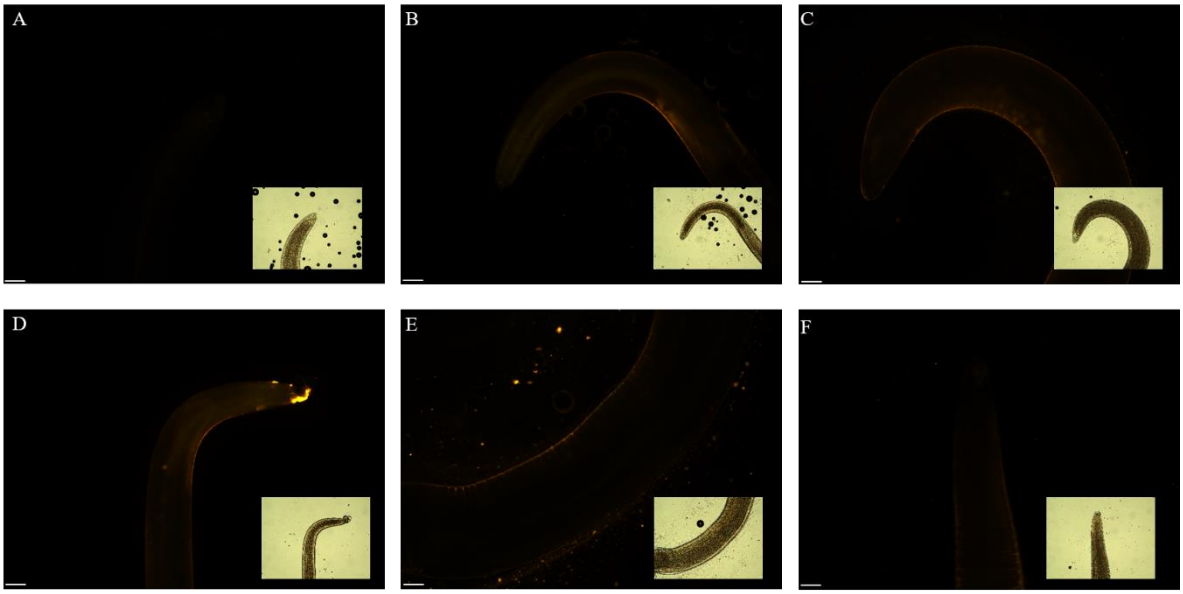

Figure S1. *Anisakis* spp. L3 cultured for 5 minutes in the presence of 0 μM (A), 1 μM (B), 4 μM (C) or 8 μM (D) 1,2-dioleoyl-sn-glycero-3-phosphoethanolamine-N-(lissamine rhodamine B sulfonyl) prior to washing, fixation with 4% paraformaldehyde and analysis using fluorescence microscopy. *Anisakis* spp. L3 cultured for 16 hours in the presence of 8 μM (E+F)) 1,2-dioleoyl-sn-glycero-3-phosphoethanolamine-N-(lissamine rhodamine B sulfonyl. Orange=Rhodamine, Scale bar = 100 μm. Corresponding bright field images are inset.

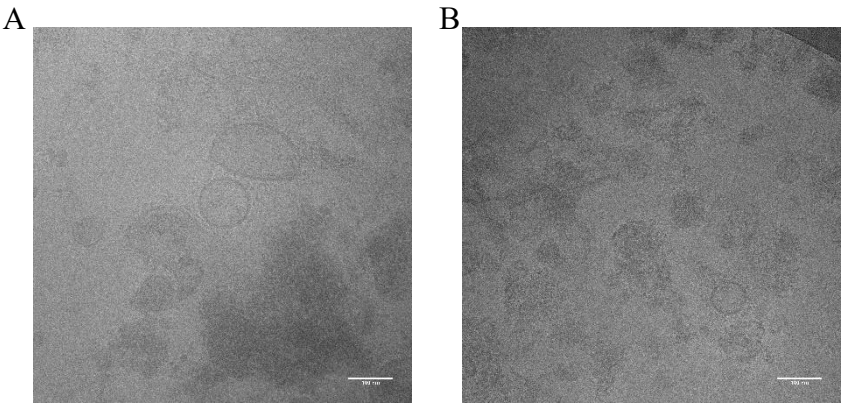

Figure S2. Cryo-TEM images of 4 μM (A) and 8 μM (B) lipid labelled vesicles. Scalebar 100 nm.